



# The potentials of *Calotropis procera* against filarial elephantiasis: an in-silico approach

Aswin Mohan<sup>1</sup> · Shanitha Shaji<sup>1</sup> · Sunitha Padmanabhan<sup>1</sup> · Shahanas Naisam<sup>2</sup> · Nidhin Sreekumar<sup>2</sup>

Received: 12 April 2021 / Accepted: 17 September 2021 / Published online: 19 October 2021  
© Indian Society for Parasitology 2021

**Abstract** Lymphatic filariasis is one of the major diseases that belong to the category of neglected tropical illness. Filarial nematodes are the cause of the disease and are transmitted to humans via blood-feeding arthropod vectors. Drugs such as Albendazole, Ivermectin and diethylcarbamazine are administered either individually or in combination to overcome the progress of the lymphatic filariasis. These drugs have some minor side effects like temporary hair loss, dizziness, nausea etc. The filarial parasites have multifunctional proteins including the Glutathione-s-transferase (GST) enzyme. This study aims at the identification of a natural molecule that has the potential to bind with the GST enzyme, which plays a major role in detoxification of endogenous electrophilic compounds. Thus the binding interrupts the detoxification process within the filarial parasite, *Brugia malayi*. A medicinal plant *Calotropis procera*, owing to its anthelmintic properties was searched for the presence of potential phytochemicals. The phytochemicals were docked against the homology modeled GST enzyme using the MOE software. The results were screened and analyzed based on the Lipinski rule of 5. N-octanoate was the phytochemical obtained based on molecular docking, subjected to molecular dynamics. These results require further in vitro and in vivo validation to consider n-octanoate as a potential drug candidate for lymphatic filariasis treatment.

**Keywords** Lymphatic filariasis · *Brugia malayi* · *Calotropis procera* · Molecular docking · Molecular dynamics

## Introduction

Lymphatic filariasis or Filariasis is one of the neglected tropical diseases caused by the nematode filarial parasites *Wuchereria bancrofti*, *Brugia malayi* and *Brugia timori*. Filariasis causes permanent limb disability and can even cause permanent malformations of several body parts (Ottesen et al. 2008). The filarial parasites are thread-like parasitic nematodes (roundworms) and are transmitted to the human host through blood-feeding arthropod vectors. The adult worms reside in specific tissues within the host where they release thread-like microfilariae into the blood. The circulating microfilariae enter the vector during blood-feeding and develop into an infective larva ready for human transmission. The intensity of the disease in the host depends on the locations of the tissue preferred by the microfilariae and matured worms. The matured worms inhabit lymph vessels, causing lymphatic inflammation and dysfunction due to blockage and host reactions and gradually lead to lymphedema and fibrosis (Stillwaggon et al. 2016). Prolonged and recurrent infection with these worms can lead to a buildup of excess tissue in the affected area, as in elephantiasis (Cross 1996).

Published articles on filariasis emphasize the importance of Glutathione-s-transferases (GST) in chronic infections. GSTs are multifunctional proteins that belong to an enzyme family which filarial parasitic worms depend for their survival in the host (Bhargavi et al. 2005). GSTs are major detoxification enzymes that neutralize cytotoxic

✉ Nidhin Sreekumar  
nidhin@accubits.com

<sup>1</sup> Dept. of Computational Biology and Bioinformatics,  
Kariavattom Campus, University of Kerala, Trivandrum,  
Kerala, India

<sup>2</sup> Accubits Invent Pvt. Ltd, The Pirates Square, Trivandrum,  
Kerala, India

compounds and protect cells and tissues from the reactive oxygen species attack. They catalyze the conjugation of Glutathione (GSH) to endogenous electrophilic compounds that are less harmful (Bhoj et al. 2020). These enzymes protect the tissue from damage caused by free radicals, superoxides and aids in the intracellular transport of non-catalytic carrier proteins (Sommer et al. 2001). GST's involvement in drug resistance and biosynthesis of arachidonic acid metabolites makes GST a more attractive target for therapeutics (Van Ommen et al. 1991). Studies prove that GST of humans are structurally different from worms and can be used as a potential target for developing anti-filarial drugs (Brophy et al. 2000).

The present drugs have poor inhibition on adult parasitic worms. Current treatment includes Mass Drug Administration of drugs such as Albendazole, Ivermectin, Doxycycline and Diethylcarbamazine etc. individually or in combination (Brophy and Pritchard 1994). Intake of these drugs shows some trivial side effects like dizziness, temporary hair loss, nausea, fever, headache, and joint pain etc. The mechanism of action and side effects of the drugs used in Filariasis treatment are presented in Table 1. This scenario makes us ponder over an alternative drug that possesses potentiality against the disease with no side-effects.

Traditional medicines from natural resources- phyto-compounds have long been promising substitutes in the treatment of various diseases. They exhibit favorable potency, bearable toxicity and curable properties. *Calotropis procera* Linn. is a common shrub mostly found as a weed around India (Iyadurai et al. 2020), attributed to warm and dry areas, the sub- Himalayan regions and the southern regions of the country. Different parts of *C. procera* have been reported to possess different therapeutic activities such as proteolytic (Atal and Sethi 1962)

antimicrobial, larvicidal (Al-Rowaily et al. 2020), nematocidal, anticancer, anti-inflammatory (Basu and Chaudhuri 1991; Kumar and Basu 1994). Its flowers possess digestive and tonic properties.

This study focuses on proposing a potent lead molecule against filarial elephantiasis from traditional medicinal plant *C. procera*. Homology modeling, Molecular docking and molecular dynamics studies are performed on a potential drug target of filarial parasite—Glutathione-S-transferase with phytocompounds retrieved from *C. procera*.

## Materials and methods

### Target selection

The sequence of Glutathione S transferase of *B. malayi* was retrieved from UniProt (UniProt ID: A0A0H5S7P0) (2021) having 208 residues and was considered for homology modeling. Homology modeling is a molecular modeling technique, which builds a 3D structure from a template homologous protein structure. In this study, the protein was modeled using an online tool—swiss model (Peitsch 1996). The sequence was uploaded in the swiss model to search for homologous protein templates. Template 5d73.1.A (structure of pi-class glutathione S-transferase of *W. bancrofti*, which was identified as the causative organism of > 90% filariasis cases) (Farrar et al. 2013) is selected from the results with the following values: GMQE: 0.95, QMEAN: – 0.11, QSQE: 1.00. The modeled structure of Glutathione S transferase of *B. malayi* has single A chain of 208 residues starting from MET to final residue GLN.

**Table 1** Drugs used in the treatment of Lymphatic filariasis, their mechanism of action and side effects

| Drug               | Mechanism of action   | Side effects  |
|--------------------|---|---|
| Diethylcarbamazine | Microfilaria to phagocytosis, Arachidonic acid metabolic pathway, cyclooxygenase pathway  | Dizziness, nausea, fever, headache, and joint pain  |
| Albendazole        | Binds to the colchicine-sensitive site of tubulin, thus inhibiting its polymerization or assembly into microtubules. It also causes degenerative alterations in the intestinal cells of the worm by diminishing its energy production, ultimately leading to immobilization and death of the parasite | Temporary hair loss, vomiting, spinning sensations, neck stiffness, and seizures              |
| Ivermectin         | Binds to the glutamate-gated chloride ion channels in invertebrate muscle and nerve cells of the microfilaria which results in hyperpolarization of the cell, leading to paralysis and death of the parasite  | Eye pain, puffy eyes, skin rash, itching, painful neck and armpits, diarrhea, rapid heartbeat |
| Doxycycline        | Inhibits translation by binding to the 16S rRNA portion of the ribosome, preventing binding of tRNA to the RNA-30S bacterial ribosomal subunit which results in the replication of bacteria and produces a bacteriostatic effect  | Nausea, vomiting, stomach cramps, sore throat, unusual weight loss                            |

In this study, the binding sites used for docking were retrieved from literature and includes Tyr7, Phe8, Gly12, Leu13, Trp 38, Lys42, Gln49, Leu50, Ser 63, His98, Thr99, Tyr 101, Thr102, Tyr106 and Val202 (Domadia et al. 2008, Kalani et al. 2014 and Mathew et al. 2011).

### Target validation

The homology modeled structure was validated using multiple tools like ERRAT, Verify3D and Procheck. (Colovos and Yeates 1993; Laskowski et al. 1993). The modeled protein was uploaded in the SAVESv6.0 (ERRAT—DOE-MBI Structure Lab UCLA) to estimate the ERRAT, Verify 3D and Procheck plots. ERRAT identifies and calculates the statistics of non-bonded interactions between different atom types and generates “the error function versus position of a 9-residue sliding window” plot based on the data from highly refined structures. Verify 3D determines the compatibility of an atomic model (3D) by using its own amino acid sequence (1D). A structural class based on the atomic model’s location and environment (alpha, beta, loop, polar, non-polar, etc.) is assigned and compared with the results of the best structures. Procheck analyzes residue-by-residue geometry and overall structure geometry (Ramachandran plot, chi1-chi2 plot, main-chain parameters, side chain parameters, residue properties, main-chain bond lengths, main chain bond angles and planar groups) of modelled structure to provide the stereochemical quality of the protein.

### Ligand structure collection

Phytochemical composition of *C. procera* were listed out from literature surveys and 47 ligand structures were retrieved from PubChem database in.sdf file format (Kim et al. 2021).

### ADME prediction

ADME (Absorption, Digestion, Metabolism and Elimination) properties of the phytochemicals were calculated using Swiss ADME. Swiss ADME calculated the ALogp, MLogP, WLogP, Molecular weight, Solubility, GI (Gastrointestinal) absorption, and blood–brain barrier permeability, PAINS (Pan Assay Interfering Compounds) of the selected phytochemicals. The canonical smiles of the phytochemicals retrieved from PubChem were given as an input for ADME prediction. Physicochemical properties of ligands were calculated using DataWarrior (Sander and Freyss 2015). The ligands were filtered under Lipinski rule of 5, mutagenicity and PAINS.

### Molecular docking

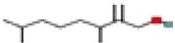


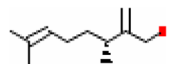

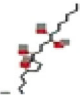





Molecular docking studies were performed in Molecular Operating Environment (MOE) (ULC 2020). The modeled structure of GST was considered as target protein and ligand molecules (13 ligands) that satisfy Lipinski rule of 5, PAINS (0 alerts) and are non-toxic in nature were considered for docking. Pre-docking procedures such as protein preparation, binding site identification, and ligand database creation were done prior to docking. The purified target structure was loaded, and the structure was prepared to resolve the issues such as H-count, charge, library, etc. (Kute and Thorat 2014). The Protonate 3D tool was used to protonate the target structure after structure preparation and default parameters were used. The binding sites were defined using the sequence editor by selecting the residues and its corresponding atoms. The selected residues were highlighted in the graphic window. A database (.mdb file format) was created for importing ligand structures into a single file in MOE. Docking was performed using the Dock application from the compute tool panel and force field OPLS AA was used for this study. The parameters set for the docking were as follows; Receptor: MOE file, Site: Selected residues, Ligand: MDB file, Method:—Placement: Triangle Matcher; score: London dG; Poses:5, Refinement: rigid receptor; score: Affinity dG; Poses: 5. A file was created explicitly for the output storage and specified in the dock parameter setting panel. Post docking evaluations were performed by analyzing each docking conformation individually. The receptor-ligand interaction analysis approach was used to analyze Hydrogen-bond interactions in favorable sites and S-score. Hydrogen bond interactions between residues of defined binding sites and phytochemicals were considered as favorable H-bond interactions.

Binding affinity calculation was performed using PyRx software by vina wizard (Dallakyan and Olson 2015), the binding affinity of ligands were estimated and analyzed for better interactions. Binding affinity is the strength of the binding interaction of a biomolecule to a ligand/ binding partner.


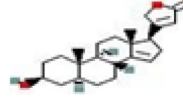
### Molecular dynamics

For molecular dynamics, GROMACS (version 2020.1), an open-source molecular dynamics software, was used (Berendsen et al. 1995). There was a separation of the docked complex into protein and ligand. The force field used was the CHARMM36 all-atom force field, and the CGenFF server supported the ligand parameters and topologies compatible with the above force field. The separated protein and ligand were developed into a complex and ligand topology and parameter files were added to

**Table 2** The list of 13 phytocompounds selected for the study

| Sl. No | Ligand   | Pub Chem ID | 2D Structure  | Mol. Wt | ALogP   | H-Donor | H-Acceptor | Toxicity    | PAINS (Pan Assay Interfering Compounds) |
|--------|--|-------------|---|---------|---------|---------|------------|-------------|---|
| 1      | 3,7-Dimethyl-2-methylene-1-octanol   | 3,023,988   |    | 4.717   | 370.525 | 1       | 3          | Non-Mutagen | 0 alerts                                |
| 2      | 1-Octanol  | 957         |    | 2.795   | 130.228 | 1       | 1          | Non-Mutagen | 0 alerts                                |
| 3      | 2-tridecanone  | 11,622      |    | 4.668   | 198.345 | 0       | 1          | Non-Mutagen | 0 alerts                                |
| 4      | 6-Octen-1-ol, 3,7-dimethyl-2-methylene-, (R)-(R)-(-)-3,7-dimethyl-2-methylene-6-octen-1-ol | 10,877,531  |    | 3.239   | 168.276 | 1       | 1          | Non-Mutagen | 0 alerts                                |
| 5      | 9-Decenoate  | 5,460,709   |    | 1.791   | 169.241 | 0       | 2          | Non-Mutagen | 0 alerts                                |
| 6      | Acetogenins  | 393,472     |  | 4.221   | 470.639 | 4       | 7          | Non-Mutagen | 0 alerts                                |
| 7      | Benzoylisolineolone  | 5,322,013   |  | 2.606   | 468.582 | 3       | 6          | Non-Mutagen | 0 alerts                                |
| 8      | Gigantin   | 4696        |  | - 0.269 | 154.12  | 1       | 4          | Non-Mutagen | 0 alerts                                |
| 9      | N-Hexadecanoate  | 504,166     |  | 4.919   | 255.416 | 3       | 4          | Non-Mutagen | 0 alerts                                |
| 10     | N-Octanoate  | 119,389     |  | 1.269   | 143.203 | 0       | 2          | Non-Mutagen | 0 alerts                                |
| 11     | Nonanoic acid, 7-methyl methyl ester   | 521,322     |  | 3.676   | 186.291 | 1       | 3          | Non-Mutagen | 0 alerts                                |

**Table 2** Continued

| Sl. No | Ligand                           | Pub Chem ID | 2D Structure  | Mol. Wt | ALogP   | H-Donor | H-Acceptor | Toxicity    | PAINS (Pan Assay Interfering Compounds) |
|--------|----------------------------------|-------------|---|---------|---------|---------|------------|-------------|---|
| 12     | Undecanoic acid                  | 8180        |  | 4.111   | 186.291 | 2       | 3          | Non-Mutagen | 0 alerts                                |
| 13     | $\beta$ -anhydroepidigitoxigenin | 10,784,500  |  | 4.142   | 356.498 | 1       | 3          | Non-Mutagen | 0 alerts                                |

**Table 3** Ligands with better interaction result with their binding affinity

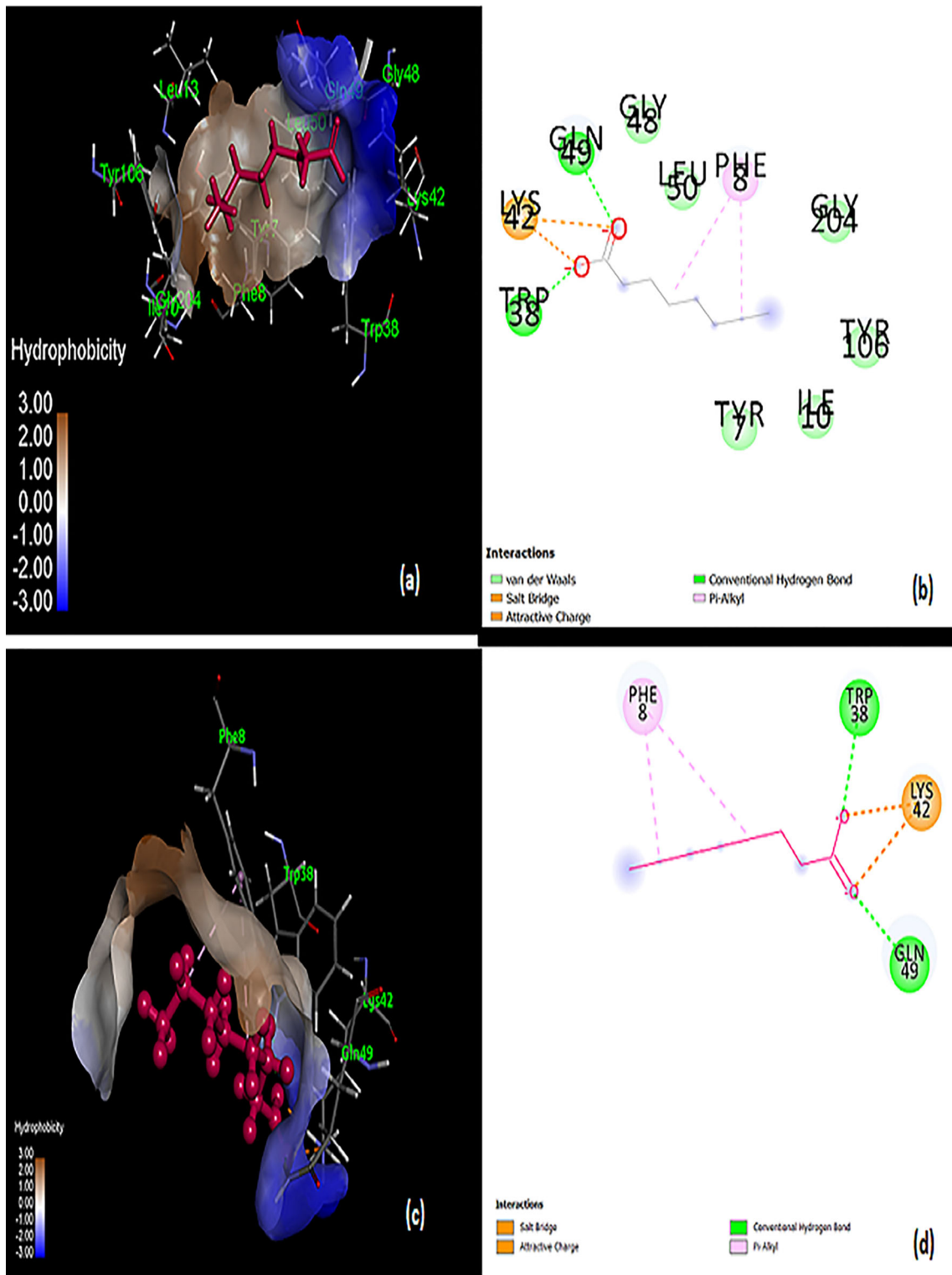
| Sl No. | Ligand   | H-Bond Interaction     | S- Score | Binding Affinity' (kcal/mol) |
|--------|--|------------------------|----------|------------------------------|
| 1      | 3,7-Dimethyl-2-methylene-1-octanol   | Tyr7, Thr102, Asn203   | 105.201  | – 4.2                        |
| 2      | 1-Octanol  | Gly12, Asp159          | 65.2532  | – 3.9                        |
| 3      | 2-tridecanone  | Gln49, Gln62           | 72.3555  | – 4.1                        |
| 4      | 6-Octen-1-ol, 3,7-dimethyl-2-methylene-, (R)-' (R)-(-)-3,7-dimethyl-2-methylene-6-octen-1-ol | Gln42, Lys91, Phe152   | 74.4469  | – 4.3                        |
| 5      | 9-Decenoate  | Gln49, Gln62           | 69.9742  | – 4.2                        |
| 6      | Acetogenins  | Tyr7, Tyr106, Arg95    | 106.044  | – 4.2                        |
| 7      | Benzoylisolineolone  | Tyr106                 | 99.2344  | – 4.1                        |
| 8      | Gigantin   | Tyr7                   | 62.3747  | – 4.1                        |
| 9      | N-Hexadecanoate  | Trp38, Lys42, Leu50    | 87.2003  | – 4.2                        |
| 10     | N-Octanoate  | Trp 38, L'ys 42, Gln49 | 54.3566  | – 4.9                        |
| 11     | Nonanoic acid, 7-methyl methyl ester   | Tyr7, Tyr106           | 65.5374  | – 4.1                        |
| 12     | Undecanoic acid  | Tyr7, Tyr106, Asn203   | 71.533   | – 4.1                        |
| 13     | $\beta$ -anhydroepidigitoxigenin   | Gln49                  | 68.2219  | – 4.1                        |

**Table 4** Binding affinity, S score and interacting residues of n-Octanoate

| Ligand      | Interacting Residues   | H-Bond Interaction     | S-Score | Binding Affinity |
|-------------|--|------------------------|---------|------------------|
| N-Octanoate | Tyr 7, Phe 8, Ile 10, Trp 38, Lys 42, Gly 48, Gln 49, Leu 50, Tyr 106, Gly 204 | Trp 38, Lys 42, Gln 49 | 54.3566 | – 4.9 kcal/mol   |

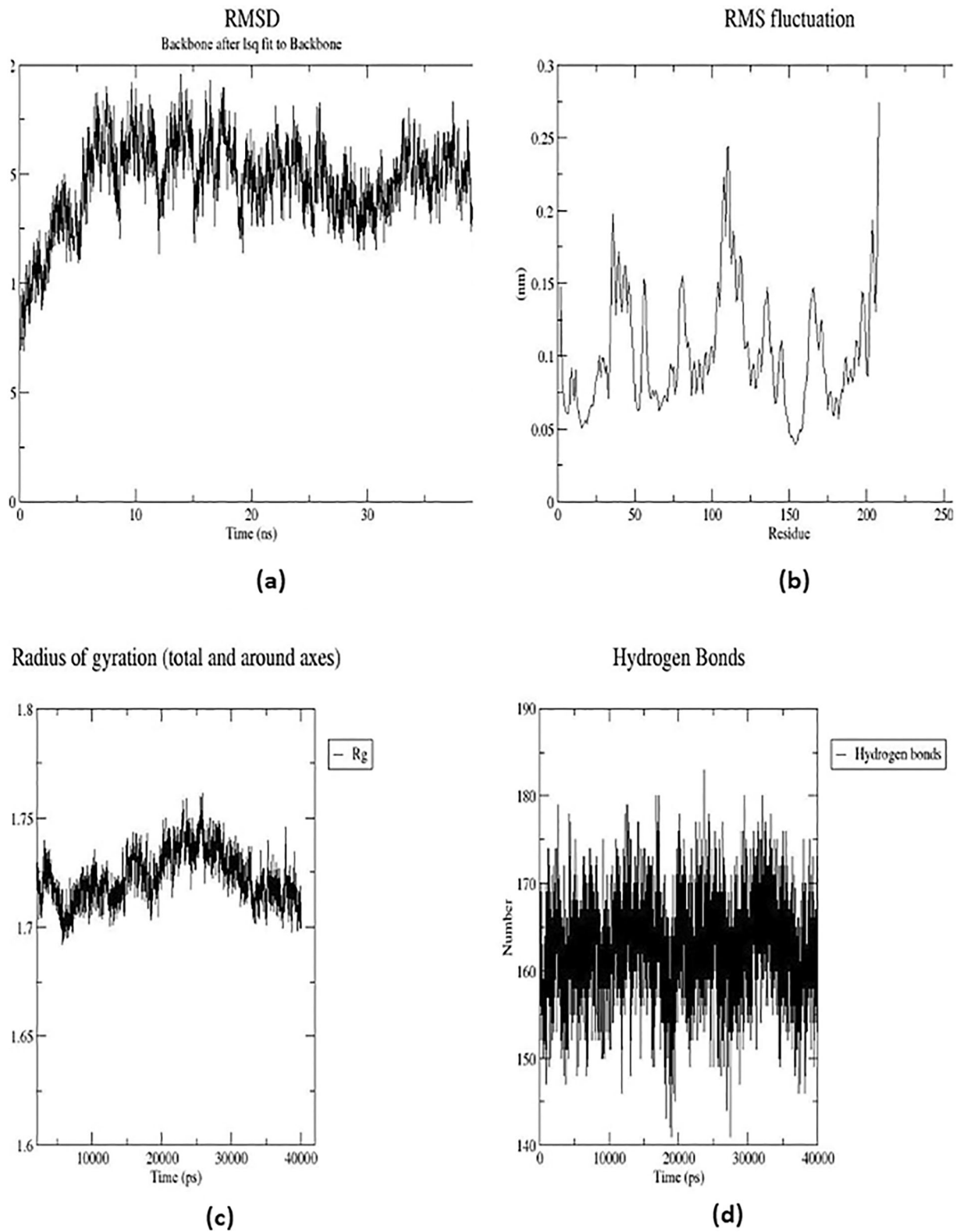
the protein topology file, resulting in the topology file of the complex. In the solvation process the complex was solvated using water. In order to prepare the complex for

energy minimization, required ions were added into the solvated complex. Energy minimization was carried out in order to bring the complex into its minimum potential



**Fig. 1** **a** Hydrophobic surface of interaction n-Octanoate with Glutathione-s-transferase, **b** 2D interactions of n-Octanoate with Glutathione-s-transferase, **c** Hydrophobic surface of interaction n-Octanoate with Glutathione-s-transferase after simulation, **d** 2D

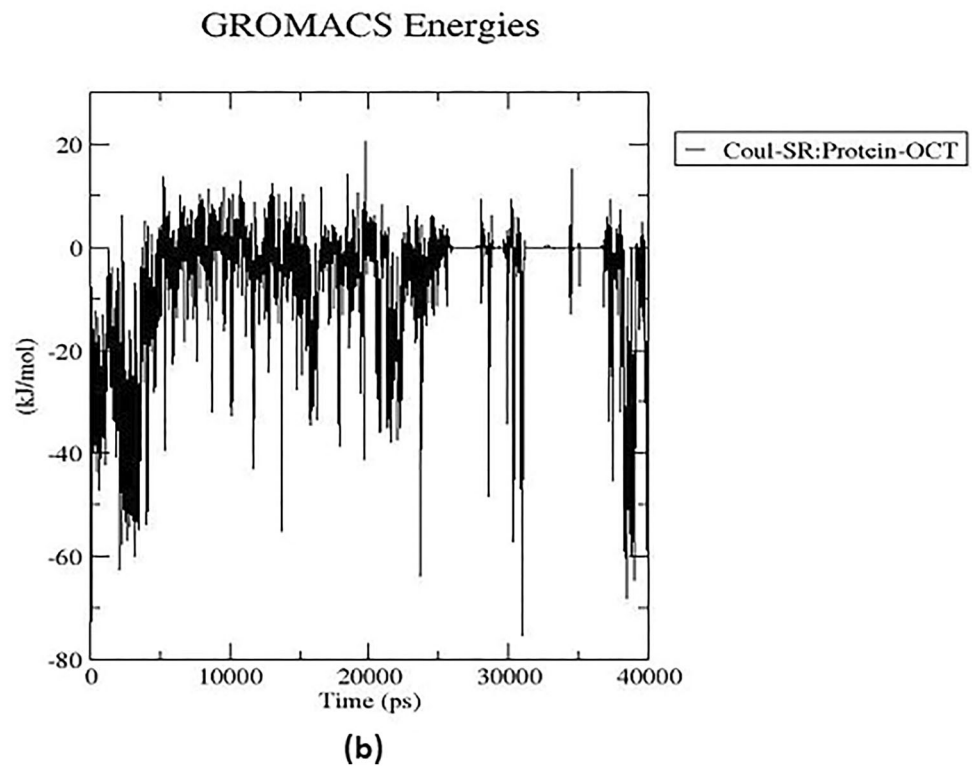
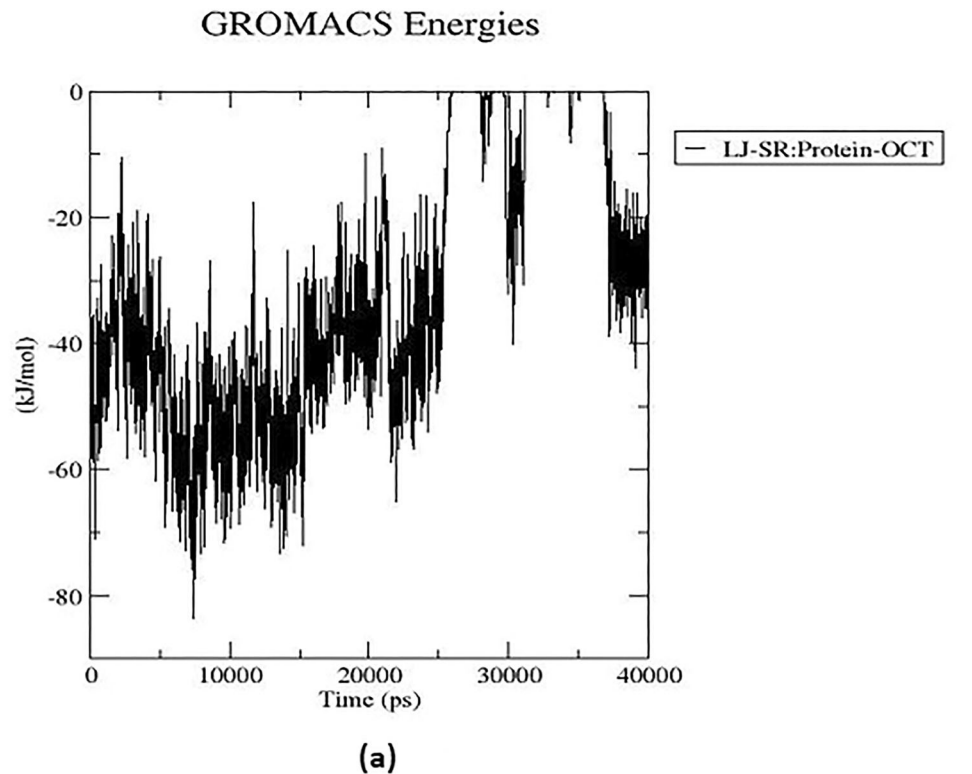
interactions of n-Octanoate with Glutathione-s-transferase after simulation



**Fig. 2** **a** RMSD plot of n-Octanoate–Glutathione-s-transferase complex, **b** RMSF plot of n-Octanoate–Glutathione-s-transferase complex, **c** RoG plot of n-Octanoate–Glutathione-s-transferase complex, **d** Number of hydrogen bonds plot Glutathione-s-transferase- system complex



**Fig. 3** **a** Lennard–Jones short-range potential energy of n-Octanoate–Glutathione-s-transferase complex, **b** Coulombic Short-range potential energy of n-Octanoate–Glutathione-s-transferase complex



energy. Restraining the ligand and treatment of temperature coupling groups was accompanied by energy minimization. The complex was regulated by equilibration of

volume- NVT ensemble (constant Number of particles, Volume, and Temperature) followed by equilibration of pressure- NPT ensemble (Number of particles, Pressure,



and Temperature). An MD simulation run for 40 ns was initiated. The trajectories of docked complexes were analyzed through 40 ns of molecular dynamics simulation. The simulated complex was analyzed for Root Mean Square Deviation, Root Mean Square Fluctuation, Radius of gyration, number of hydrogen bonds and interaction energy.

## Result and discussion

Glutathione-s-transferase (GST) is the multifunctional protein that comprises major detoxification enzymes. It mainly helps the organism's macromolecules to stay intact from the attack of electrophiles and they catalyze the conjugation of Glutathione to the electrophiles. They are mostly found in the cytosol and in addition to catalyzing the conjugation to electrophiles they perform some peroxidase and isomerase activities. Since it has a significant role in the parasite worm's life cycle, it can be considered as a drug target.

Sequence from UniProt was used to search for homologous protein templates, and template 5d73.1.A was selected as it had the following parameter values; GMQE (Global Model Quality Estimation): 0.95, QMEAN: – 0.11, QSQE (Quaternary Structure Quality Estimate): 1.00 showed that template 5d73.1.A was a suitable model.

ERRAT plots show a quality factor of 93.9547 which shows that the model has a good quality (Messaoudi et al. 2013). 96.14% of the residues had passed the average 3D-1D score  $\geq 0.2$  when validated by Verify3D (Ullah et al. 2012). In the Ramachandran plot, 0% residues were found in the disallowed region inferring that the model has a good secondary structure (Waghmare et al. 2016).

Glutathione-s-transferase was taken as the target and phytocompounds structures from the plant *C. procera* were taken as ligands for docking studies. The molecular properties and ADMET descriptors of 47 ligands were calculated and were screened under Lipinski's rule of 5, PAINS, and toxicity. Out of 47, only 13 ligands satisfied Lipinski's rule of 5, PAINS (0 alerts), and non-mutagenic property (Table 2).

The Molecular Operating Environment software was used for molecular interaction study. The protein preparation was done for eliminating the water molecules and adding explicit hydrogens. Binding sites were selected from the literature survey, defined as follows Tyr7, Phe8, Gly12, Leu13, Trp 38, Lys 42, Gln49, Leu50, Ser63, Arg95, His98, Thr99, Tyr101, Thr102, Tyr106 and Val202. Ligands were written into a single database file in MOE and the ligands and protein were subjected to docking.

The docking result had 374 poses and top-scored conformations (13 poses) per ligand were selected based on

H-bond interactions and S score and also binding affinity of the ligands towards the receptor was calculated (Table 3). The compound with desired hydrogen bond interactions (hydrogen bond in the defined binding sites) and least binding affinity were selected from Table 3. Phytocompound n-Octanoate showed desired hydrogen bond interaction with the given binding sites such as Trp 38, Lys 42, Gln49, have higher binding affinity and exhibit druggable characteristics (Table 4). The 2D plot of interactions and hydrophobic interactions of n-Octanoate with Glutathione-s-transferase was studied (Fig. 1a and b). This ligand has the least binding affinity; hence it has the highest binding stability with the target protein (Glutathione-s-transferase). The ligand n-Octanoate resulted in better docking scores and satisfied Lipinski's rule of 5.

The docked complex was subjected to molecular dynamics using GROMACS. The temperature was equilibrated at 300 K and the pressure was equilibrated at 1 bar for a time for MD run, 40 ns. Figure 1c and d depicts the hydrogen bond interactions of the ligand with the protein and residues Lys 42 and Trp 38 maintained hydrogen bonds with the ligand n-Octanoate after the simulation. i.e., two out of three hydrogen bonds were still intact through the simulation until the end of simulation which points that the compound n-Octanoate is a successful binder with the receptor protein. The RMSD (Root Mean Square Deviation) (Fig. 2a) plot and RMSF (Root mean square fluctuation) plot (Fig. 2b) of the complex after simulation were obtained. The RMSD deviates in between 0.1 and 0.2 nm, stabilizes at 0.15 nm from 20 ns up to the end of simulation, showing less deviation in RMSD (Cob-Calan et al. 2019). The part of the protein that fluctuates mostly during the period of simulation can be understood from RMSF, infers in the flexibility of protein in a binding state. Residue 208 shows the greater fluctuation among the total protein residues. The Radius of Gyration defines the rigidity of the system, greater degree of fluctuation results in the inconsistency throughout the simulation shows the compactness of the system. The RoG of the complex fluctuated in between 1.7 and 1.75 m, with an average of 1.725 nm and found more fluctuating at 25 ns inferring in the higher compactness/ rigidity of the system (Fig. 2c) (Turner et al. 2019). The total number of hydrogen bonds in the complex throughout the simulation was also estimated and a maximum of 182 hydrogen bonds, a minimum of 140 hydrogen bonds, an average of 165 bonds were found to be in the complex (Fig. 2d). Interaction energies of the complex including Lennard-Jones short-range and Coulombic short-range potential energies were calculated. The Lennard-Jones short-range potential energy of the complex was found to be – 31.5848 kJ/mol with a total drift of 53.4165 kJ/mol (Fig. 3a) and Coulombic shot-

range potential energy,  $-6.63557$  kJ/mol with a total drift of  $9.61891$  kJ/mol (Fig. 3b).

In the future, several factors will be playing a prominent role in the prevalence of lymphatic filariasis. A study suggests that changing patterns of climate will be interfering in the spread of parasitic diseases. A re-emergence of parasitic diseases is possible due to global warming and its associated changes in the environment (Rodó et al. 2013; Wu et al. 2016). The migration to metropolitan cities and international trade/Global market can be a potential channel to spread transmittable diseases (Irvine et al. 2015). Mass Drug Administration (MDA) is controlling the disease to an extent (Kalyanasundaram et al. 2020). Mutation of parasitic nematodes can decrease the efficiency of MDA (Kwarteng et al. 2016). Additional measures like morbidity management, vector control and surveillance must be employed more efficiently to minimize the spread of the disease (Famakinde 2018) and (Irvine et al. 2015) Vector control, reducing human—vector contact and improvising the standard of living can be crucial in eliminating filariasis (Rebollo and Bockarie 2017).

## Conclusion

The docking studies using Glutathione-S- transferase of *B. malayi* as the target intend to find a potent drug candidate for Lymphatic Filariasis. Phytocompounds from the plant *C. procera* were used as the ligand molecules. The phytocompound n-Octanoate have shown promising results and can be considered for the purpose. This ligand has H-bond interaction with the binding sites of GST. N-octanoate showed the least binding energy  $-4.9$  kcal/mol from the screened phytocompound database. Further in vitro and in vivo studies can be used to confirm these candidates as a potential drug that can be used against Filariasis.

**Acknowledgements** I am grateful to Dr. Achuthsankar S. Nair, Head of the Department, Department of Computational Biology and Bioinformatics, University of Kerala for rendering all the facilities for the completion of the work. I am particularly thankful to Mr. Vinod M. P., Ms. Chinchu E. R., Mr. Ashish Sudharshan, Ms. Roshny Prasad, Dept. of Computational Biology & Bioinformatics, University of Kerala for the support and encouragement

**Author contributions** Optional: please review the submission guidelines from the journal whether statements are mandatory.

**Funding** Not applicable.

**Declarations**

**Conflicts of interest** The authors declare that they have no conflicting financial interests.

## References

- Al-Rowaily SL, Abd-ElGawad AM, Assaeed AM, Elgamal AM, Gendy AE-NGE, Mohamed TA, Dar BA, Mohamed TK, Elshamy AI (2020) Essential oil of *Calotropis procera*: comparative chemical profiles, antimicrobial activity, and allelopathic potential on weeds. *Molecules* 25(21):5203
- Atal C, Sethi P (1962) Proteolytic activity of some indian plants. *Planta Med* 10:77–90
- Basu A, Chaudhuri AKN (1991) Preliminary studies on the anti-inflammatory and analgesic activities of *Calotropis procera* root extract. *J Ethnopharmacol* 31:319–324
- Berendsen HJC, van der Spoel D, van Drunen R (1995) GROMACS: a message-passing parallel molecular dynamics implementation. *Comput Phys Commun* 91(1–3):43–56
- Bhargavi R, Vishwakarma S, Murty US (2005) Modeling analysis of GST (glutathione-S-transferases) from *Wuchereria bancrofti* and *Brugia malayi*. *Bioinformation* 1:25
- Bhoj PS, Bahekar S, Khatri V, Singh N, Togra NS, Goswami K, Chandak HS, Dash D (2020) Role of glutathione in chalcone derivative induced apoptosis of *Brugia malayi* and its possible therapeutic implication. *Acta Parasitol* 66:406–415
- Brophy PM, Pritchard DI (1994) Parasitic helminth glutathione S-transferases: an update on their potential as targets for immuno- and chemotherapy. *Exp Parasitol* 79:89–96
- Brophy PM, Campbell AM, van Eldik AJ et al (2000)  $\beta$ -Carbonyl substituted glutathione conjugates as inhibitors of *O. volvulus* GST2. *Bioorg Med Chem Lett* 10:979–981
- Cob-Calan NN, Chi-Uluac LA, Ortiz-Chi F, Cerqueda-García D, Navarrete-Vázquez G, Ruiz-Sánchez E, Hernández-Núñez E (2019) Molecular docking and dynamics simulation of protein  $\beta$ -tubulin and antifungal cyclic lipopeptides. *Molecules* 24(18):3387
- Cross JH (1996) Filarial nematodes. *Med Microbiol*, 4th edn
- Dallakyan S, Olson AJ (2015) Chemical biology. *Chem Biol Methods Protoc* 1263:220–243
- Domadia PN, Bhunia A, Sivaraman J et al (2008) Berberine targets assembly of *Escherichia coli* cell division protein FtsZ. *Biochemistry* 47:3225–3234
- Famakinde DO (2018) Mosquitoes and the lymphatic filarial parasites: research trends and budding roadmaps to future disease eradication. *Trop Med Infect Dis* 3:4
- Farrar J, Hotez PJ, Junghanss T et al (2013) Manson's tropical diseases E-Book. Elsevier health sciences, Amsterdam
- Irvine MA, Reimer LJ, Njenga SM et al (2015) Modelling strategies to break transmission of lymphatic filariasis-aggregation, adherence and vector competence greatly alter elimination. *Parasit Vectors* 8:1–19
- Iyadurai R, Gunasekaran K, Jose A, Pitchaimuthu K (2020) *Calotropis* poisoning with severe cardiac toxicity A case report. *J Fam Med Prim Care* 9(8):4444
- Kalani K, Kushwaha V, Sharma P et al (2014) In vitro, in silico and in vivo studies of ursolic acid as an anti-filarial agent. *PLoS ONE* 9:e111244
- Kalyanasundaram R, Khatri V, Chauhan N (2020) Advances in vaccine development for human lymphatic filariasis. *Trends Parasitol* 36(2):195–205
- Kim S, Chen J, Cheng T, Gindulyte A, He J, He S, Li Q, Shoemaker BA, Thiessen PA, Yu B, Zaslavsky L, Zhang J, Bolton EE (2021) PubChem in 2021: new data content and improved web interfaces. *Nucleic Acids Research*, [online] 49(D1), pp.D1388–D1395. Available at: <https://academic.oup.com/nar/article/49/D1/D1388/5957164>
- Kumar VL, Basu N (1994) Anti-inflammatory activity of the latex of *Calotropis procera*. *J Ethnopharmacol* 44:123–125

- Kute SS, Thorat SD (2014) A review on various software development life cycle (SDLC) models. *Int J Res Comput Commun Technol* 3:778–779
- Kwarteng A, Ahuno ST, Akoto FO (2016) Killing filarial nematode parasites: role of treatment options and host immune response. *Infect Dis Poverty* 5:1–6
- Laskowski RA, MacArthur MW, Moss DS, Thornton JM (1993) PROCHECK: a program to check the stereochemical quality of protein structures. *J Appl Crystallogr* 26:283–291
- Mathew N, Srinivasan L, Karunan T et al (2011) Studies on filarial GST as a target for antifilarial drug development—in silico and in vitro inhibition of filarial GST by substituted 1, 4-naphthoquinones. *J Mol Model* 17:2651–2657
- Messaoudi A, Belguith H, Ben HJ (2013) Homology modeling and virtual screening approaches to identify potent inhibitors of VEB-1  $\beta$ -lactamase. *Theor Biol Med Model* 10:1–10
- Ottesen EA, Hooper PJ, Bradley M, Biswas G (2008) The Global programme to eliminate lymphatic filariasis: health impact after 8 Years. *PLoS Negl Trop Dis* 2:e317
- Peitsch MC (1996) ProMod and Swiss-Model: Internet-based tools for automated comparative protein modelling. *Biochem Soc Trans* 24(1):274–279
- Rebollo MP, Bockarie MJ (2017) Can lymphatic filariasis be eliminated by 2020? *Trends Parasitol* 33:83–92
- Rodó X, Pascual M, Doblas-Reyes FJ et al (2013) Climate change and infectious diseases: can we meet the needs for better prediction? *Clim Change* 118:625–640
- Sander T, Freyss J (2015) Mütevazı von Korff, christian rufener. datawarrior: kimya için veri görselleştirme ve analizini destekleyen açık kaynaklı bir Program. *J Chem Inf Model* 55:460–473
- Sommer A, Nimtz M, Conradt HS et al (2001) Structural Analysis and Antibody Response to the Extracellular Glutathione S-Transferases from *Onchocerca volvulus*. *Infect Immun* 69:7718–7728
- Stillwaggon E, Sawers L, Rout J et al (2016) Economic costs and benefits of a community-based lymphedema management program for lymphatic filariasis in Odisha State, India. *Am J Trop Med Hyg* 95:877–884
- Turner M, Mutter ST, Kennedy-Britten OD, Platts JA (2019) Molecular dynamics simulation of aluminium binding to amyloid- $\beta$  and its effect on peptide structure. *PLoS ONE* 14(6):e0217992
- ULC CCG (2020) Molecular operating environment (MOE), 2019.01
- Ullah M, Ghosh T, Ishaque N, Absar N, Hira J (2012) A Bioinformatics Approach for Homology Modeling Binding Site Identification of Triosephosphate Isomerase from *Plasmodium falciparum* 3D7. *J Young Pharm* 4(4):261–266
- (2021) UniProt: the universal protein knowledgebase in 2021. *Nucleic Acids Res* 49:D480–D489. <https://doi.org/10.1093/nar/gkaa1100>
- Van Ommen B, Ploemen J, Bogaards JJP et al (1991) Irreversible inhibition of rat glutathione S-transferase 1–1 by quinones and their glutathione conjugates. *Struct Act Relatsh Mech Biochem J* 276:661–666
- Waghmare S, Buxi A, Nandurkar Y et al (2016) In silico sequence analysis, homology modeling and function annotation of leishmanolysin from *Leishmania donovani*. *J Parasit Dis* 40:1266–1269
- Wu X, Lu Y, Zhou S et al (2016) Impact of climate change on human infectious diseases: Empirical evidence and human adaptation. *Environ Int* 86:14–23

**Publisher's Note** Springer Nature remains neutral with regard to jurisdictional claims in published maps and institutional affiliations.